Spectroscopy of Hydrothermal Reactions. 9. IR and Raman Spectroscopy of Hydrolysis and Self-Reaction of Cyanamide and Dicyandiamide at 130−270 °C and 275 bar

A. J. Belsky and T. B. Brill*

Department of Chemistry and Biochemistry, University of Delaware, Newark, Delaware 19716

Received: February 25, 1998; In Final Form: April 7, 1998

The hydrothermolysis reaction scheme of cyanamide, NH_2CN, and dicyandiamide, $(NH_2)_2CNCN$, applies to the role of these compounds in chemical evolution and to their destruction in aqueous waste streams by hydrothermal methods. Real-time IR spectroscopy with an optically accessible flow cell and Raman spectroscopy with a stopped-flow cell were used at set temperatures of 130−270 °C and a pressure of 275 bar to specify the details of the pathway. Rate constants and Arrhenius parameters were determined for the major steps, i.e., hydrolysis of cyanamide, conversion of cyanamide into dicyandiamide, hydrolysis of dicyandiamide, and hydrolysis of the guanylurea intermediate. Previously reported hydrolysis kinetics for guanidine and urea at hydrothermal conditions were used to complete the kinetic scheme. In addition, the apparent equilibrium constants for deprotonation of cyanamide and the protonation of dicyandiamide and its monoanion were determined. The conversion of dicyandiamide to ammeline and the hydrolysis of ammeline were observed by Raman spectroscopy at longer times than were used for the kinetic analysis. A relatively complete and consistent reaction scheme now exists for the cyanamide−dicyandiamide system at hydrothermal conditions.

Introduction

Cyanamide, NH_2CN, occurs in interstellar space[1] and readily dimerizes to dicyandiamide $(NH_2)_2CNCN$, which is believed to have a role in chemical evolution.[2,3] Both are formed when a representative prebiotic atmosphere of NH_3, HCN, CH_4, and H_2O is exposed to UV or e-beam radiation.[3] The resulting dicyandiamide functions as a dehydration coupling agent that links glucose and adenosine to H_3PO_4 and thereby forms glucose-6-phosphate and adenosine-5′-phosphate, respectively.[2] Cyanamide and dicyandiamide also have commercial application as intermediates in the formation of pharmaceuticals (e.g., Tagamet), pesticides, fungicides, herbicides, and various polymers.[4] The carbodiimide linkage like that of these compounds is present in an additive to prevent hydrolysis of the nerve agent VX. They are also used in fabric treatments and flame retardants for textiles[5] and are burning-rate suppressants in solid rocket propellants.[6,7]

The natural synthesis of cyanamide and its conversion to the biosynthetic coupling agent dicyandiamide in H_2O may have contributed to chemical evolution since prebiotic times. Questions remain, however, as to whether these compounds can exist and how they react in H_2O at elevated temperatures and pressures. As components in commercial, industrial, and military products, cyanamide and dicyandiamide may show up in waste streams whose remediation by wet-air oxidation[8] and supercritical water oxidation[9,10] might be contemplated. Although reactions of cyanamide and dicyandiamide have been extensively studied this century,[11−13] the behavior in H_2O at high temperature and pressure, i.e., hydrothermal conditions, has only recently been outlined (Figure 1).[14] To understand better the hydrothermolysis reaction schemes and kinetics of aqueous cyanamide and dicyandiamide under these extreme

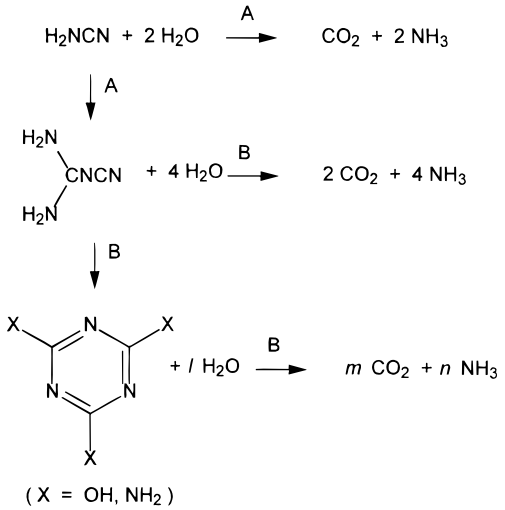

Figure 1. Reaction pathway developed previously (ref 14) by postreaction analysis of hydrothermolysis of cyanamide and dicyandiamide in the batch mode. Reactions labeled A dominated below 175 °C, whereas those labeled B become evident above 175 °C.

conditions, real-time analysis by IR and Raman spectroscopy was undertaken in the 130−270 °C range under 275 bar. The critical point of pure water is 374 °C and 221 bar. In situ IR spectroscopic characterizations of aqueous solutions at high temperature and pressure have been applied with success to other environmentally and commercially important compounds, such as urea,[15,16] ammonium carbonate,[16,17] guanidinium nitrate,[15] carbohydrazide,[18] hydroxylammonium nitrate,[17,19] ammonium thiocyanate,[20] malonic acid,[21] and formic acid.[22] This work extends and quantifies reaction details beyond that possible with batch reaction methods. The behavior of cyanamide and dicyandiamide differs significantly from the forementioned compounds in that, in addition to hydrolysis and decomposition

* Corresponding author.

S1089-5639(98)01296-1 CCC: $15.00
Published on Web 05/15/1998

to lower molecular-weight compounds, self-reaction to higher molecular-weight compounds is also evident.[14] This behavior is well-known in the thermolysis schemes of neat cyanamide and dicyandiamide,[11−13,23,24] but the details differ in the presence of H_2O at hydrothermal conditions.[14] The pathway and kinetics of these relatively complex reactions are described in greater detail herein by the combination of IR and Raman spectroscopy and flow cells and separate studies of the intermediates. The possible role of cyanamide and especially dicyandiamide in chemical evolution seems plausible based on its degree of kinetic inertness at hydrothermal conditions and its hydrolytic conversion to other molecules that are components of essential biochemical molecules. They will degrade rapidly, however, at the conditions used in hydrothermally based waste remediation technologies, which frequently exceed 300 °C.

Experimental Section

A small-scale flow reactor spectroscopy cell[15,16] constructed of 316 stainless steel (SS) with sapphire windows was sealed by compressing gold-foil washers at each interface. The fluid flowed in the flat duct that was formed between two sapphire windows and a slot in the gold washer that separated the windows. The path length of the cell (thickness of the flat duct) was determined to be 30 ± 5 μm by the absorbance of a known concentration of aqueous CO_2 flowing through the cell.[16] The system controls have been described[16] with the exception that a control program written in Visual Basic is now used to maintain the pressure at 275 ± 1 bar, to regulate the reaction temperature to ± 1 °C, to control the flow rate as desired in the 0.054−1.00 mL/min range, and to collect the IR spectra. These flow rates result in residence times in the range 3−60 s. A single liquid phase was maintained at all times as evidenced by the absence of IR modes for gaseous CO_2 and H_2O in the spectrum.

Cyanamide (hereafter Cy), dicyandiamide (hereafter Dicy), urea, guanidinium carbonate, and guanylurea sulfate were obtained from Aldrich Chemical Co. Ammeline was obtained from Pfaltz and Bauer. Solutions were then made from Milli-Q H_2O that had been sparged with Ar to remove atmospheric gases. Because Dicy is less soluble than Cy, the spectroscopy studies were conducted with concentrations of 0.50 *m* Cy (*m* = mol/kg) and 0.25 *m* Dicy.

A Nicolet 60SX FTIR spectrometer with a liquid-N_2-cooled MCT-B detector was used for real-time spectral measurements. Thirty-two spectra were summed at 4 cm^{-1} resolution (10 s collection time) at each chosen flow rate and temperature. These spectra were normalized with background spectra of pure H_2O recorded at the same conditions. The reactants and many of the products have IR-active fundamental modes in the band-pass above the sapphire cutoff at about 1800 cm^{-1} and below the H_2O cutoff at about 3000 cm^{-1}. Figure 2 shows the IR spectra of aqueous Cy and Dicy at room temperature. ν_a(NCN) of Dicy[26] at 2200 and 2184 cm^{-1} can be detected at a concentration above 0.001 *m*; however, in the presence of a large excess of Cy, these modes become difficult to resolve and the detection limit is somewhat raised. The absorbance maximum of ν(CN) of Cy in H_2O is at 2245 cm^{-1} with a shoulder at 2224 cm^{-1}. Aqueous CO_2 is a reaction product whose asymmetric stretch at 2343 cm^{-1} has been thoroughly characterized at the reaction conditions.[16] A potential intermediate is the cyanate ion, OCN^-, whose asymmetric stretch at 2165 cm^{-1} overlaps the fundamental of Dicy. In these reactions it would be possible to detect OCN^- only in relatively high concentrations, which never occurred. The concentrations of each species during the reaction were determined from Beer's law plots from IR spectra of standard solutions of the pure compounds.

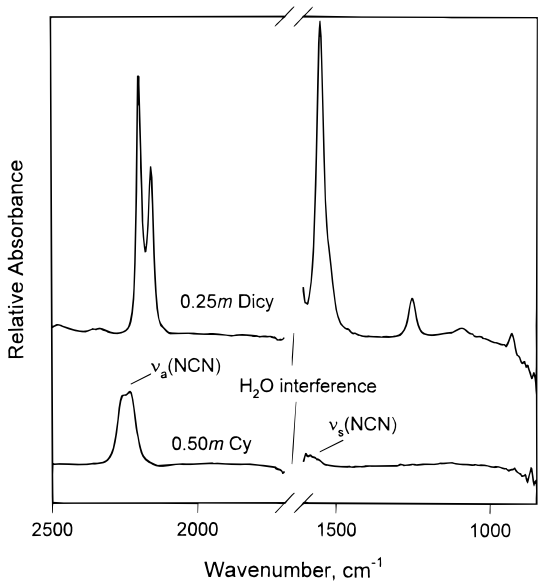

Figure 2. IR spectra of aqueous Cy and Dicy recorded at 23 °C in a transmission cell with ZnSe windows. Diagnostic modes for each exist in the 2000−2500 cm^{-1} range.

To investigate the kinetics of reactions, flow rates were used such that plug−flow conditions could be assumed to exist in the cell.[15,27] The resulting degree of conversion was 30% or less. The true residence time was obtained by dividing the internal volume of the cell (entrance tube and flat duct), which was 0.0604 cm^3, by the mass flow rate (volume flow rate × ρ_T). The mass flow rate was used because the density of H_2O, ρ_T, changes with temperature (e.g., $\rho_{130°C} = 0.94$ g/cm^3, $\rho_{270°C} = 0.80$ g/cm^3 at a constant pressure of 275 bar). The IR spectrum was resolved into the individual components at each reaction condition using Peakfit software (Jandel Scientific). Four-parameter Voigt functions were employed for this procedure. Three sets of data were recorded at each reaction condition to establish the average concentration and the standard deviation. In subsequent kinetic modeling of Cy it was found that smoothing of concentration−time data with second-, third-, or fourth-order regressions, as appropriate, was useful because the IR modes of Cy had relatively low intensity. Smoothing was not necessary for the Dicy data. A weighted least-squares regression was used for determination of the rate and Arrhenius parameters. Appropriate care was taken when converting the standard deviation of the rate constants into log space as is required to determine the Arrhenius parameters.[28]

Raman spectroscopy was not used for kinetic measurements but provided an additional method to identify species and validate the reaction pathways. A stopped-flow cell was constructed from 316 SS with sapphire windows and gold foil compression seals (Figure 3). The internal volume of this cell was 0.22 cm^3. The Raman backscattering was collected from the solution by using a Kaiser Optical Systems dispersive Raman spectrometer with a thermoelectrically cooled CCD detector and a 50 mW diode-pumped, frequency-doubled, Nd:YAG laser for excitation at 532 nm. Five scans (10 s each) were recorded and averaged to give the spectrum. The concentrations change slightly during the Raman spectral collection, but this created no extra issues in the analysis because no quantitative analysis was made. The wider band-pass and longer reaction times available with Raman spectroscopy expanded and complemented

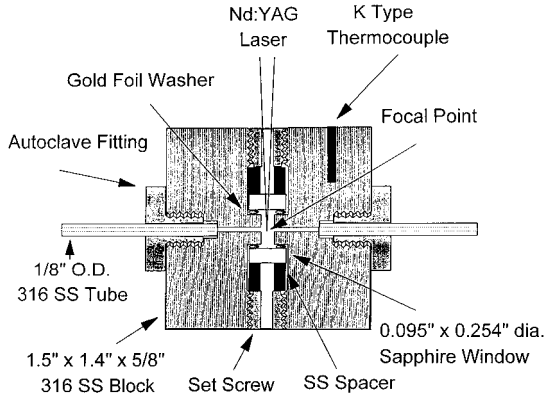

Figure 3. Cross section of the stopped-flow cell used for Raman spectroscopy of the solutions at elevated temperature and 275 bar. The cell was surrounded with heating blocks and wrapped with insulating tape.

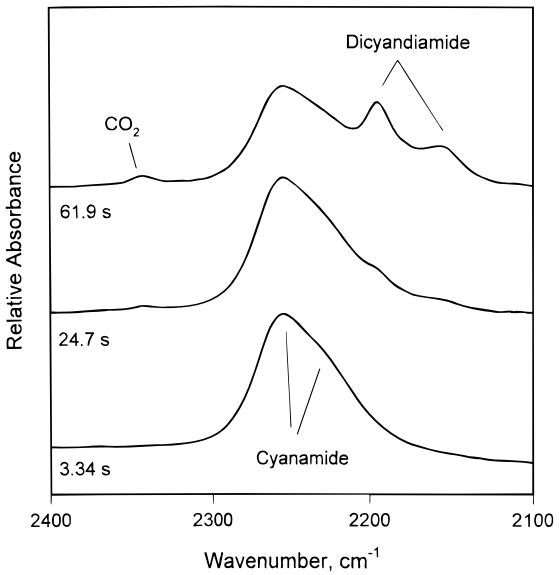

Figure 4. Selected IR spectra at different residence times showing the conversion of 0.5 *m* Cy to Dicy at 150 °C and 275 bar.

the view of the reaction pathway obtained from IR spectroscopy. The additional species were identified to be urea by its 994 cm^{-1} shift with a concentration detection limit of about 0.04 *m*, guanidine by its 1008 cm^{-1} shift with a detection limit of about 0.01 *m*, ammeline (X = OH and $2NH_2$ in Figure 1) by its 693 cm^{-1} ring deformation mode determined to have an approximate detection limit of 0.003 *m*, and guanylurea by its 978 cm^{-1} shift with an approximate detection limit of 0.015 *m*.

The ionization equilibrium constants for Cy, $Dicy^-$, and Dicy were needed in the kinetics model and were determined from the temperature dependence of the pH of aqueous solutions of each compound. $Dicy^-$ was made by titrating Dicy with one equivalent of NaOH. An Orion 330 pH meter with an Ag/AgCl perpHect electrode was used with the log *R* function that corrects for the pH change of water over the temperature range used.

Hydrothermolysis Pathway of Cyanamide. In this section the details of the reactions labeled "A" in Figure 1 were uncovered. Batch reaction of aqueous Cy in a sealed SS tube below 175 °C with reaction times less than 15 min predominately produced Dicy.[14] Some Cy hydrolysis to CO_2 and NH_3 was detected at these conditions as well. It is possible to follow these reactions by IR spectroscopy in the flow reactor with sapphire windows because, as is shown in Figure 2, Cy and

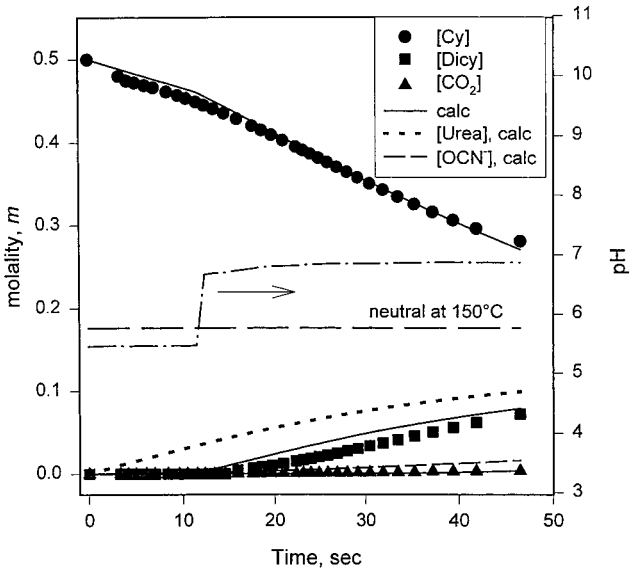

Figure 5. Concentration profiles of the species shown that were used in kinetic modeling of the hydrothermolysis of 0.5 *m* cyanamide at 150 °C and 275 bar. The computed pH change during the reaction is also shown.

Dicy have −C≡N stretching fundamentals in the 2100−2300 cm^{-1} range, and aqueous CO_2 can be followed by its asymmetric stretching mode at 2343 cm^{-1}. The spectra obtained with the flow reactor IR cell in real time (Figure 4) are in essential agreement with A steps of the batch mode results (Figure 1).[14] The self-reaction of Cy to form Dicy is apparent along with formation of a small amount of CO_2. The formation of CO_2 indicates the occurrence of hydrolysis and would be accompanied by the formation of NH_3 whose IR modes are outside the spectral band-pass available.

The reaction pathway for hydrothermolysis of Cy shown in eqs 1−5

$$\mathrm{Cy} + \mathrm{H_2O} \xrightarrow{k_1} (\mathrm{NH_2})_2\mathrm{CO} \quad (1)$$

$$(\mathrm{NH_2})_2\mathrm{CO} + \mathrm{H_2O} \rightarrow \mathrm{CO_2} + 2\mathrm{NH_3} \quad (2)$$

$$\mathrm{Cy} + \mathrm{H_2O} \overset{K_C}{\rightleftharpoons} \mathrm{Cy^-} + \mathrm{H_3O^+} \quad (3)$$

$$\mathrm{Cy} + \mathrm{Cy^-} \xrightarrow{k_2} \mathrm{Dicy^-} \quad (4)$$

$$\mathrm{Dicy^-} + \mathrm{H_2O} \overset{K_{D^-}}{\rightleftharpoons} \mathrm{Dicy} + \mathrm{OH^-} \quad (5)$$

accounts for the time dependence of Cy, Dicy, and CO_2 in the 130−170 °C range (Figure 5) under 275 bar and also builds on previous reports of the characteristics of Cy in the normal liquid range of H_2O.[29−34] The production of H_3O^+ by eq 3 and OH^- by eq 5 is charge-balanced in H_2O solution.

Equation 1 accounts for the fact that the Cy concentration in Figure 5 decreases before Dicy or CO_2 is detected. Therefore, a relatively stable intermediate must be present that is IR-silent in the band-pass of the sapphire windows. This intermediate is plausibly urea, $(NH_2)_2CO$, in that urea has no IR absorbances in the 1800−3000 cm^{-1} band-pass, is formed by both acid[29−31,34] and base[28,33] hydrolysis of cyanamide in the normal liquid range of H_2O, and is sufficiently inert to survive at 130−170 °C on the time scale used for these reactions before eq 2 ensues.[15,16] We searched for urea in the Raman spectrum under similar conditions because the calculated concentration (vide infra)

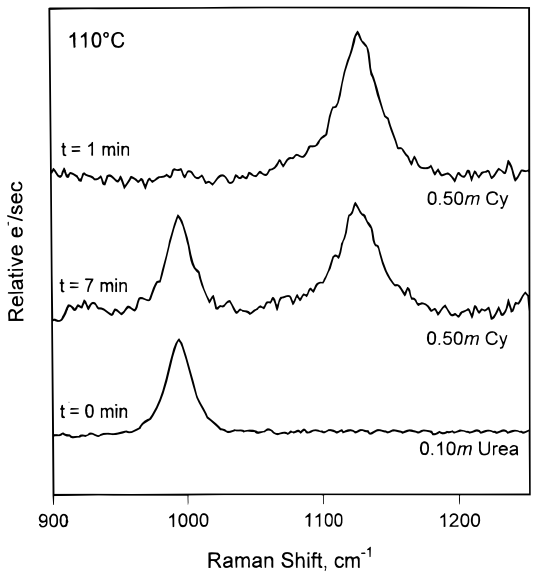

Figure 6. Raman spectra of reacting aqueous Cy in the stopped-flow batch mode showing evidence of urea when compared with an authentic sample of aqueous urea.

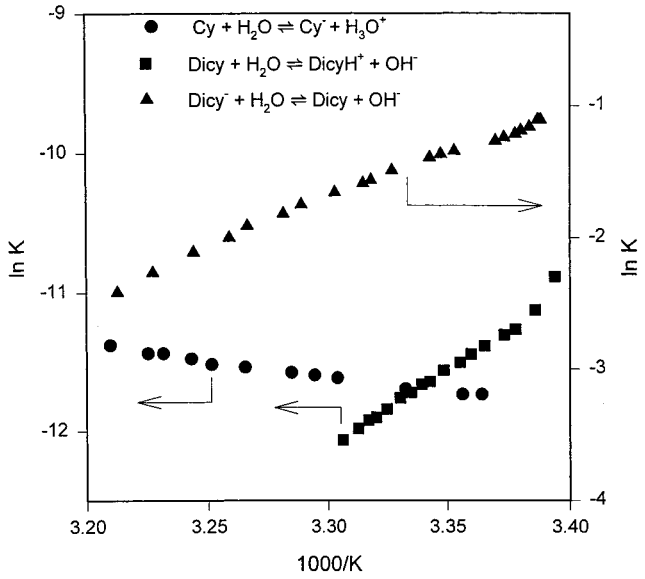

Figure 7. van't Hoff plot for the ionic equilibria of Cy (eq 3), $Dicy^-$ (eq 5), and Dicy (eq 8) in H_2O.

should be detectable by its 994 cm^{-1} shift. Indeed, as shown in Figure 6, there is evidence of urea in the Raman spectrum of the reacting solution of Cy at 175 °C at about 275 bar. Therefore, the rate of eq 1 can be determined from the concentration−time dependence of Cy before CO_2 or Dicy is detected.

The hydrolysis of urea to CO_2 and NH_3 by eq 2 has been previously studied in detail by IR spectroscopy using the same flow reactor with both sapphire and diamond windows.[15,16] The intermediate species NH_4OCN is not detected in the present work owing to its expected low concentration (given the low urea concentration) and the fact that the diagnostic OCN^- stretching mode (2165 cm^{-1}) overlaps the strongly IR-active CN stretch of Dicy (Figure 4). The previously determined kinetics of eq 2[15,16] were used, therefore, in the kinetics model discussed below. Equation 2 is very important in the mechanism in that the products CO_2 and NH_3 together initially raise the pH slightly and then buffer the solution. Most of the facts discussed here about eqs 1 and 2 are invisible in the batch reaction mode.

The existence of the equilibrium eq 3 is indicated by the fact that cyanamide is slightly acidic in H_2O solution.[32] ΔH for the ionization equilibrium, K_C (eq 3), was estimated many years ago[32] to be roughly 42 kJ/mol. K_C was redetermined here as an apparent equilibrium quotient from the temperature dependence of the pH in the 22−40 °C range. From the slope in Figure 7, $\Delta H°$ for eq 3 was determined to be 0.62 kJ/mol. K_C was incorporated into the kinetic model described below by using the iso-Coulombic method, which takes into account the changing value of K_W [36] and improves the approximation of independence of ΔH with temperature.

As the pH rises slightly owing to eq 2, the equilibrium eq 3 shifts to the right. This produces more Cy^-, which is a reactant for eq 4. The occurrence of eqs 4 and 5 becomes evident in the appearance of Dicy in Figures 4 and 5. Equations 4 and 5 together were previously known,[29,37] but the kinetics in the hydrothermal regime have not been determined. The apparent equilibrium constant K_D^- for eq 5 was not found in the literature and, therefore, was determined in the same manner as described above for eq 3 but by using the NaDicy salt. A value of $\Delta H° = -1.95$ kJ/mol was obtained (Figure 7) and was used in the kinetics model described below. The rate constant for eq 4 (k_2) can then be determined from the rate of formation of Dicy. No other products were detected by IR or Raman spectroscopy in the initial 1 min of reaction in the 130−175 °C range.

Kinetics of Hydrothermolysis of Cyanamide. The rate constants for eqs 1 and 4 were determined from eqs 1 and 3−5 by first accounting for the pH change during the reaction by using the charge balance (eq 6).

$$[Cy^-] + [OH^-] + [HCO_3^-] + [Dicy^-] = [H^+] + [NH_4^+] + [DicyH^+] \quad (6)$$

Parametrizing eq 6 in terms of the single unknown variable $[H^+]$ leads to eq 7:

$$\frac{K_C[Cy]}{[H^+]} + \frac{K_W}{[H^+]} + \frac{K_{CO_2}[CO_2]}{[H^+]} + \frac{K_D[Dicy^-]}{[H^+]} = [H^+] + \frac{K_N N_T}{K_N + \frac{K_W}{[H^+]}} \quad (7)$$

To obtain eq 7, the appropriate value of K_W at each of the reaction conditions was used;[35] the concentrations of $DicyH^+$ and CO_3^{2-} were assumed to be negligible because of the pH of the solution; $N_T = [NH_3] + [NH_4^+]$; and $K_N = [NH_4^+][OH^-]/[NH_3]$. When eq 7 was solved at each time and temperature for $[H^+]$, the running value of the pH shown in Figure 5 was obtained. An accounting of $[H^+]$ at all times is necessary for two reasons. First, eq 4 is affected by the pH through eq 3, and second, the total $[CO_2]$ is the amount of CO_2 observed in the IR spectrum[16] plus the amount in the form of HCO_3^-, which is $[H^+]$-dependent. The value of K_{CO_2} at the appropriate temperatures[38] was used in eq 7. The initial absence of CO_2 or Dicy in the reaction enables k_1 to be calculated from a plot of ln[Cy] vs time, assuming, as is reasonable, that this reaction is a pseudo-first-order process. Table 1 lists the resulting rate constants. The rate constant for eq 4 (k_2) was determined from the rate of formation of Dicy, which is expected to have second-order kinetic behavior. Table 1 gives the values. In reality

TABLE 1: Rate Constants for Hydrothermolysis of 0.5 *m* Cy (Eqs 1 and 4) at 275 bar

temp, °C	$k_1 \times 10^3$, s^{-1}	k_2, kg mol^{-1} s^{-1}
130	1.2 ± 0.8	
140	1.8 ± 0.7	5.5
150	3.4 ± 2.9	20.5
160	5.3 ± 2.4	55.1 ± 7.7
170	21 ± 6	114 ± 14
180	37 ± 17	168 ± 48

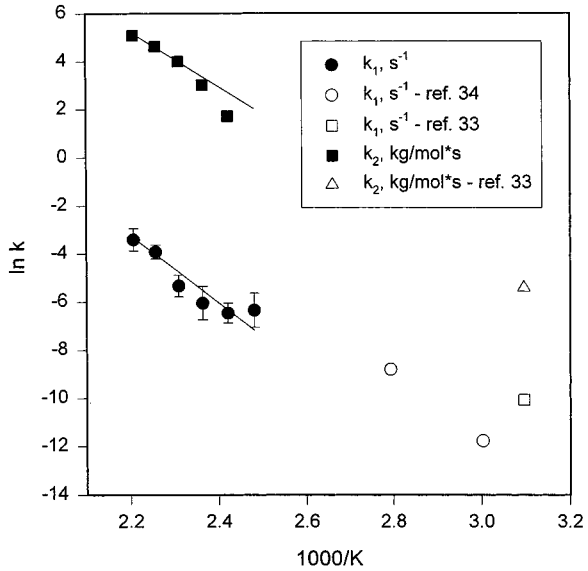

Figure 8. Arrhenius plots for k_1 (eq 1) and k_2 (eq 4) for the hydrothermal regime showing also the previously reported rates at lower temperatures. The error bars for k_2 are equal to or smaller than the symbols except for the two lowest temperatures, which are single determinations. The lines shown are weighted least-squares fits.

TABLE 2: Arrhenius Constants for Cy and Dicy

	E_a, kcal/mol	ln(A, s^{-1})
k_1 (this work)	27.8 ± 2.9	27.61 ± 3.43
k_1 (ref 34)	36	42
k_2 (this work)	22.9 ± 1.4	30.62 ± 1.68[a]
k_3 (this work)	17.46 ± 0.68	12.2 ± 0.6
k_3 (ref 40)	26.8	24.2
k_3 (ref 39)	9.1 ± 0.1	3.21 ± 0.43
k_4 (this work)	21.53 ± 0.42	18.59 ± 0.57
k_4 (ref 40)	44.3	49.5

[a] Units are kg mol^{-1} s^{-1}.

the fact that only a maximum of about 30% conversion of Cy was modeled makes it speculative to specify the reaction order. Other reaction orders fit the data about as well within the error of the measurement. The model predictions compared with the experimental data are shown in Figure 5 and agree well. The calculated concentration for urea is in line with the Raman spectra shown in Figure 6. The concentration calculated for OCN^- is below the limit of detection in the presence of Dicy. The main uncertainty in this model is the assumption that ΔH of eqs 3 and 5 is independent of temperature.

Arrhenius parameters for eqs 1 and 4 were calculated from the plots in Figure 8. Table 2 contains the resulting values. Also shown in Figure 8 are several rate measurements reported by others for Cy in acid solution in the normal liquid range of H_2O.[33,34] Clearly, eq 4 (k_2) is faster than eq 1 (k_1), but the low concentration of the Cy^- reactant for eq 4 disguises this fact in the concentration profiles of Figure 5. The previously reported rate constants agree in the sense that $k_2 > k_1$ and very roughly can be extrapolated from the rates in the hydrothermal regime.

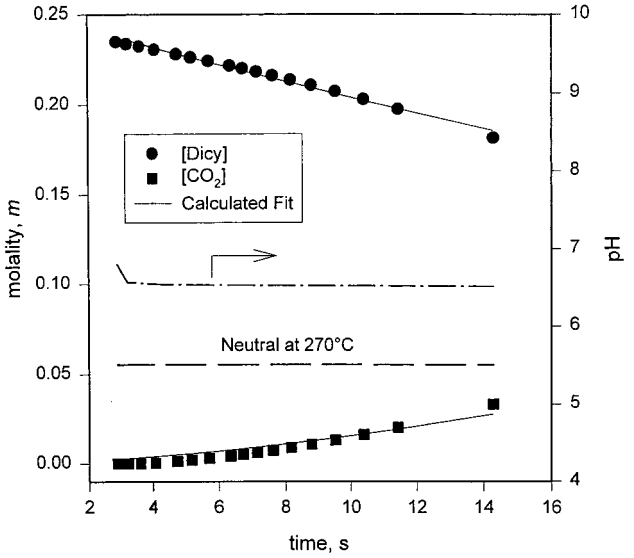

Figure 9. Concentration−time profiles of Dicy and CO_2 at 270 °C under 275 bar determined in the IR flow cell. Model calculations of the concentrations and the pH trend are shown.

Hydrothermolysis Pathway of Dicyandiamide. The details of hydrothermolysis of Dicy, which are primarily the reactions labeled "B" in Figure 1, were elucidated in much greater detail by characterizing aqueous Dicy spectroscopically in real time while in the reacting state. To this end 0.25 *m* Dicy and several important intermediates were examined at 210−270 °C under 275 bar in the IR flow cell and at 225 °C in the stopped-flow cell by dispersive Raman spectroscopy. The concentration−time profiles for Dicy and CO_2, which are the only observable species in the IR spectral band-pass of the cell, are shown in Figure 9. Other species are present in the reaction and were characterized by the behavior of solutions starting with these species.

After extensive study eqs 8−14 were found to account for the details of the IR and Raman spectra at the hydrothermal conditions.

$$\mathrm{Dicy} + \mathrm{H_2O} \overset{K_{D^+}}{\rightleftharpoons} \mathrm{DicyH^+} + \mathrm{OH^-} \quad (8)$$

$$\mathrm{Dicy} + \mathrm{H_2O} \xrightarrow{k_3} \mathrm{Gu} \quad (9)$$

$$\mathrm{Gu} + \mathrm{H_2O} \xrightarrow{k_4} \mathrm{G} + \mathrm{NH_3} + \mathrm{CO_2} \quad (10)$$

$$\mathrm{G} + \mathrm{H_2O} \rightarrow \mathrm{U} + \mathrm{NH_3} \quad (11)$$

$$\mathrm{U} + \mathrm{H_2O} \rightarrow \mathrm{CO_2} + 2\mathrm{NH_3} \quad (12)$$

$$\mathrm{Dicy} + \mathrm{NH_3} + \mathrm{CO_2} \rightarrow \mathrm{Am} + \mathrm{H_2O} \quad (13)$$

$$\mathrm{Am} + 5\mathrm{H_2O} \rightarrow 3\mathrm{CO_2} + 5\mathrm{NH_3} \quad (14)$$

Gu is guanylurea [$(NH_2)_2CN(H)C(O)NH_2$], G is guanidine, U is urea, and Am is ammeline (Figure 1, where X = OH and $2NH_2$). Equation 8 was included because an aqueous solution of Dicy is slightly basic and it is needed to maintain the charge balance in the kinetics analysis of Dicy discussed below. K_{D^+} was determined by measuring the pH of a solution of Dicy as a function of temperature. $\Delta H°$ for eq 8 was determined from Figure 7 to be −3.16 kJ/mol. Dicy is the predominant species in the solution and is proposed to hydrolyze and form Gu as indicated by earlier work.[39−42] Gu is consumed relatively

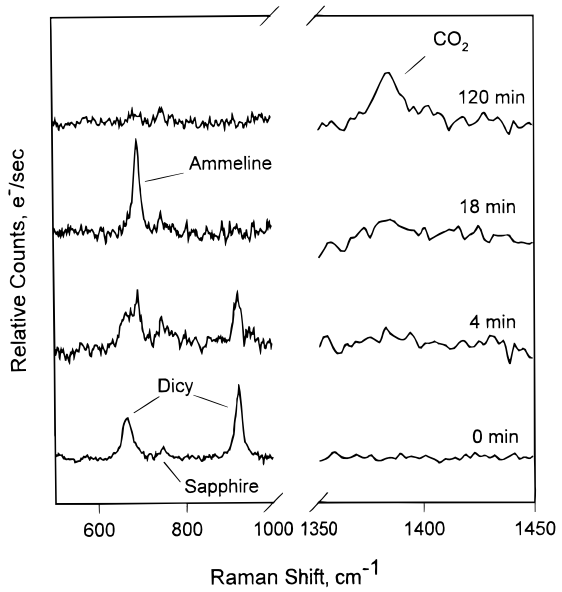

Figure 10. Raman spectra showing the conversion of aqueous Dicy to Am and Am to CO_2 in the stopped-flow cell at 225 °C under 275 bar.

rapidly by eq 10, which is also a known reaction.[39−41] Consistent with this is the fact that we were unable to detect Gu by the Raman-active mode at 978 cm^{-1}, which was determined to have a detection limit of about 0.015 *m*. Equations 9 and 10 are known reactions,[39,40,43] and eq 10 could be detected with Raman spectroscopy in a 0.1 *m* solution of guanylurea at 130 °C. The product G of eq 10 is also not expected to be detected at the reaction conditions used for Dicy based on the rate of eq 11, which has been reported previously in the hydrothermal regime.[15] As noted in the Cy section above, the kinetics of eq 12 are also known in this temperature and pressure range[15,16] and are needed to account completely for the amount of CO_2 at any time or temperature. That is, in the early stage of the reaction studied before eqs 13 and 14 become apparent, the total amount of CO_2 is determined by the rates of eqs 10−12. By use of the rates for eqs 11 and 12 and the total amount of CO_2 produced, the rate of eq 10 can be calculated, as is discussed further below. All of these features were used in modeling the concentration−time profiles of Dicy and CO_2 shown in Figure 9. Equation 10 plays a nontrivial role in the mechanism because the production of CO_2 and NH_3 initially lowers the pH of the Dicy solution slightly and then buffers against further changes (see the running pH profile Figure 9).

Equations 13 and 14 are complicating side reactions of Dicy hydrolysis at longer times whose details were examined qualitatively with the stopped-flow Raman cell. Figure 10 shows Raman spectra of an aqueous solution of Dicy in which conversion to Am is detected by the presence of the ring deformation mode at 693 cm^{-1}. None of the other OH and NH_2 substituent combinations of the *s*-triazine ring (Figure 1) were detected. This result contrasts with the previous batch reactor data with postreaction analysis[14] where all possible substituent combinations were found in somewhat random ratios. Moreover, the Am scattering intensity in Figure 10 was not consistently reproducible, which suggests that Am probably sticks to the reactor wall at hydrothermal conditions. This tendency is consistent with the fact that less cyclic azine precipitate could be recovered from hydrolysis of Dicy in an SS batch reactor as the surface area of the reactor was increased. Hydrolysis of Am by eq 14 is observed at longer times, as is shown in Figure 10 by the disappearance of Am and the appearance of CO_2.

TABLE 3: Rate Constants for Hydrothermolysis of 0.25 *m* of Dicy (Eqs 9 and 10) at 275 bar

temp, °C	$k_3 \times 10^3$, s^{-1}	$k_4 \times 10^3$, s^{-1}
210	2.6 ± 1.2	28 ± 14
220	3.6 ± 1.1	46 ± 25
230	6 ± 1.6	38 ± 13
240	6.9 ± 0.9	66 ± 58
250	9.5 ± 1.4	77 ± 64
260	14 ± 1.1	130 ± 77
270	19 ± 1.9	

Kinetics of Hydrothermolysis of Dicyandiamide. The rate constants for eqs 9 (k_3) and 10 (k_4) were obtained from the rate expressions for eqs 9−12. To solve this problem, a running account of $[OH^-]$ was necessary and was obtained from the charge balance eq 15 for the Dicy solution.

$$[OH^-] + [HCO_3^-] = [NH_4^+] + [DicyH^+] + [H^+] + [GuH^+] + [GH^+] \quad (15)$$

Conversion of eq 15 into the single $[OH^-]$ unknown yields eq 16,

$$[OH^-] + \frac{K_{CO_2}[CO_2][OH^-]}{K_W} = \frac{K_N N_T}{K_N + [OH^-]} + \frac{K_{D^+}[Dicy]}{[OH^-]} + \frac{K_W}{[OH^-]} \quad (16)$$

where K_N, N_T, and K_{D^+} were defined above. G and Gu are slightly basic, but their concentrations are very small, and so their protonated forms were dropped from eq 15. A knowledge of $[OH^-]$ at each time and temperature thus permits the total CO_2 concentration to be defined as the CO_2 observed plus that contained in HCO_3^-. $[CO_2]$ and [Dicy] are experimental observables, and values of K_W at the experimental conditions[35] are used. A plot of ln[Dicy] vs time yields the pseudo-first-order rate constant (k_3) for the disappearance of Dicy by eq 9. As was the case for Cy, the relatively low degree of conversion of Dicy precludes a firm specification of the reaction order in this way, but pseudo-first order is consistent with the form of eq 9. The total rate of CO_2 formation in the early stage depends on the rates of eqs 10−12. Since rate constants have been separately determined for eqs 11 and 12,[15,16] the rate of eq 10 (k_4) can be determined. The values of k_3 and k_4 are given in Table 3. The model predictions are compared with the experimental data in Figure 9. The calculated concentrations of Gu and G were always below the limit of detection, which is consistent with the fact that they could not be detected by Raman spectroscopy. No kinetic data for eqs 14 or 15 were obtained because of experimental difficulties in quantifying the Raman spectra in Figure 10 with sufficient accuracy.

Arrhenius parameters for eqs 9 (k_3) and 10 (k_4) were calculated from the plots shown in Figure 11. The values are given in Table 2. Figure 11 also contains the Arrhenius plot for the conversion of U[15,16] as well as previously reported rate constants for base (NaOH) hydrolysis of Dicy measured at lower temperatures and times longer than 9 h.[40] Reasonable agreement exists between k_4 at lower and higher temperatures, but extrapolation of k_3 between the two ranges reveals that the presence of added base accelerates eq 9. In separate experiments we compared the rate of disappearance of Dicy in the presence of NaOH in the tube batch reactor and found that it does, indeed,

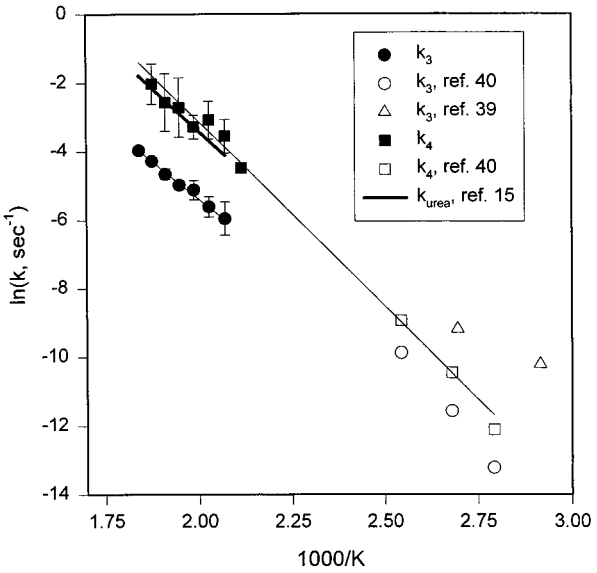

Figure 11. Arrhenius plots for k_3 (eq 9) and k_4 (eq 10) determined in the hydrothermal regime along with comparisons with previously reported rates at lower temperatures. Also shown is the rate of hydrolysis of urea in the hydrothermal regime.

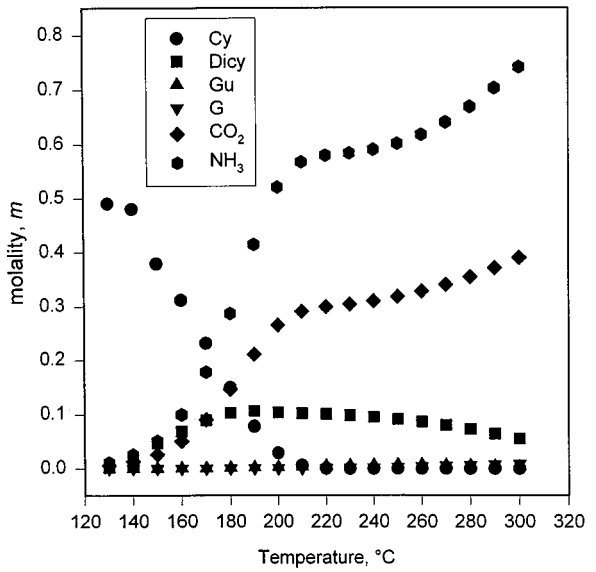

Figure 12. Concentrations of the main species during hydrothermolysis of Cy after 10 s of reaction as a function of temperature under 275 bar.

accelerate rapidly above pH = 12. This finding is consistent with the fact that Dicy is amphoteric (Figure 7), so that ionized as well as neutral forms of Dicy may participate in eq 9. The similarity of the rates of hydrolysis for Gu and U (Figure 11) suggests that the rate-determining step is the same for both compounds, e.g., probably nucleophilic attack by H_2O on the electropositive carbonyl carbon atom.

Conclusions

This work provides reaction details and several individual rate constants for the complex hydrothermolysis schemes of Cy and Dicy that were only qualitatively outlined previously by batch reaction and ex situ analysis.[14] The reaction schemes for Cy (eqs 1−5) and Dicy (eqs 8−12) can be merged to provide the prospective shown in Figure 12, where the main components in the solution after 10 s of reaction are shown as a function of temperature. The side reaction of Dicy to form Am contributes insignificantly at these conditions. For the purpose of waste stream remediation in hydrothermal and supercritical water, these compounds can be expected to convert mainly to CO_2 and NH_3 before the nominal operating temperature of the reactor is reached. In the context of Dicy as a dehydration coupling agent in chemical evolution, the pressure and temperature conditions used here are representative of those in deep-sea hydrothermal vents[44,45] and reveal that Dicy is sufficiently hydrolytically stable to be a potentially active agent. Several of the hydrolysis intermediates, such as guanidine and urea, are also components of molecules that are also essential to chemical evolution.

Acknowledgment. We are grateful to the U.S. Army Research Office for support of this work on DAAL03-92-G-0174 (R. W. Shaw, Program Manager).

References and Notes

(1) Turner, B. E.; Kislyakov, A. G.; Liszt, H. S.; Kaifu, N. *Astrophys. J.* **1975**, *201*, L149.
(2) Steinman, G.; Lemmon, R. M.; Calvin, M. *Proc. Natl. Acad. Sci. U.S.A.* **1964**, *2*, 27.
(3) Schimpl, A.; Lemmon, R. M.; Calvin, M. *Science* **1965**, *147*, 49.
(4) Forgione, P. S. In *Ullman's Encyclopedia of Industrial Chemistry*; VCH: Weinheim, Germany, 1987; Vol. A8, p 139.
(5) Costa, L.; Camino, G. *J. Calorim., Anal. Therm. Thermodyn. Chim.* **1986**, *17*, 213.
(6) Roberts, J. A.; Mangum, M. G. Air Force Rocket Propulsion Laboratory Report AFRPL-TR-84-038; September 1984.
(7) Stoner, C. E., Jr.; Brill, T. B. *Combust. Flame* **1991**, *83*, 302.
(8) Mishra, V. S.; Mahajani, V. V.; Joshi, J. B. *Ind. Eng. Chem. Res.* **1995**, *34*, 2.
(9) Savage, P. E.; Gopalan, S.; Mizan, T. I.; Martino, C. J.; Brock, E. E. *AIChE J.* **1995**, *41*, 1723.
(10) Tester, J. W.; Holgate, H. R.; Armellini, F. J.; Webley, P. A.; Killilea, W. R.; Hong, G. T.; Barner, H. E. In *Emerging Technologies in Hazardous Waste Management III*; Tedder, D. W., Pohland, F. G., Eds.; ACS Symposium Series 518; *American Chemical Society*, Washington, D.C., 1993; p 35.
(11) Baughen, A. E. *Can. Chem. Proc. Ind.* **1944**, *28*, 805.
(12) Bann, B.; Miller, S. A. *Chem. Rev.* **1958**, *58*, 131.
(13) Pankratov, V. A.; Chesnokova, A. Z. *Russ. Chem. Rev.* **1989**, *58*, 879.
(14) Belsky, A. J.; Li, T. J.; Brill, T. B. *J. Supercrit. Fluids* **1997**, *10*, 201.
(15) Schoppelrei, J. W.; Kieke, M. L.; Wang, X.; Klein, M. T.; Brill, T. B. *J. Phys. Chem.* **1996**, *100*, 14343.
(16) Kieke, M. L.; Schoppelrei, J. W.; Brill, T. B. *J. Phys. Chem.* **1996**, *100*, 7455.
(17) Schoppelrei, J. W.; Kieke, M. L.; Brill, T. B. *J. Phys. Chem.* **1996**, *100*, 7463.
(18) Schoppelrei, J. W.; Brill, T. B. *J. Phys. Chem. A.* **1997**, *101*, 2298.
(19) Schoppelrei, J. W.; Brill, T. B. *J. Phys. Chem. A.* **1997**, *101*, 8598.
(20) Maiella, P. G.; Brill, T. B. *Inorg. Chem.* **1998**, *37*, 454.
(21) Maiella, P. G.; Brill, T. B. *J. Phys. Chem.* **1996**, *100*, 14352.
(22) Maiella, P. G.; Brill, T. B. *J. Phys. Chem.*, in press.
(23) May, H. *J. Appl. Chem.* **1959**, *9*, 340.
(24) Takimoto, M.; Funakawa, T. *Kogyo Kagaku Zasshi* **1963**, *66*, 797.
(25) Davies, M.; Jones, W. J. *Trans. Faraday Soc.* **1958,** *54*, 1454.
(26) Jones, W. J.; Orville-Thomas, W. J. *Trans. Faraday Soc.* **1959**, *55*, 193.
(27) Cutler, A. H.; Antal, M. J., Jr.; Jones, M., Jr. *Ind. Eng. Chem. Res.* **1988**, *27*, 691.
(28) Cvetanovic, R. J.; Singleton, D. L. *Int. J. Chem. Kinet.* **1977**, *9*, 481.
(29) Hetherington, H. C.; Braham, J. M. *J. Am. Chem. Soc.* **1923**, *45*, 824.
(30) Sullivan, M. J.; Kilpatrick, M. L. *J. Am. Chem. Soc.* **1945**, *67*, 1815.
(31) Kilpatrick, M. L. *J. Am. Chem. Soc.* **1947**, *69*, 40.
(32) Kameyama, N. *40th American Electrochemical Society Meeting*; Lake Placid, NY, 1921; p 131.
(33) Buchanan, G. H.; Barsky, G. *J. Am. Chem. Soc.* **1930**, *52*, 195.
(34) Eloranta, J. *Suom. Kemistil. B* **1960**, *33*, 152.
(35) Marshall, W. L.; Franck, E. U. *J. Phys. Chem. Ref. Data* **1981**, *10*, 295.
(36) Lindsay, W. T., Jr. *Proc. Int. Conf. Eng. W. Pa.* **1980**, *41*, 284.

(37) Grube, G.; Nitsche, P. *Angew. Chem.* **1914**, *27*, 386.
(38) Butler, J. N. *Carbon Dioxide Equilibria and Their Applications*; Lewis Publications: Chelsea, MI, 1991.
(39) Niaz, M. A.; Khan, A. A. *Ind. J. Chem.* **1991**, *30A*, 144.
(40) Eloranta, J. *Suom. Kemistil. B* **1960**, *33*, 193.
(41) Caro, N.; Grossmann, H. *Chem.−Ztg.* **1909**, *33*, 734.
(42) Davis, T. L. *J. Am. Chem. Soc.* **1921**, *43*, 699.
(43) Davis, T. L. *J. Am. Chem. Soc.* **1921**, *43*, 2230.
(44) Rona, P. A., Bostrom, K., Laubier, L., Smith, K. L., Eds. *Hydrothermal Processes at Sea Floor Spreading Centers*; Plenum: New York, 1984.
(45) Haymon, R. M.; McDonald, K. C. *Am. Sci.* **1985**, *73*, 441.